EXPERIMENTAL OVERVIEW OF SPIN EFFECTS IN HADRONIC INTERACTIONS AT HIGH ENERGIES

ALESSANDRO BRAVAR
*Institut für Kernphysik, Johannes Gutenberg Universität, Mainz*
*J. J. Becher Weg 45, D-55099 Mainz, Germany*
*E-mail: alessandro.bravar@cern.ch*

## 1 Introduction

Experiments using polarized beams and/or polarized targets have been actively pursued during the past four decades at various laboratories in the world, and unexpected *spin effects* have been observed in a number of scattering processes. The largest set of data, however, comes from experiments where the beams and the targets were both unpolarized, and the polarization of produced hyperons has been measured through their self-analyzing parity violating decays.

The discovery of a large negative polarization, transverse to the production plane, in $\Lambda^0$ inclusive production in 1976 [1] came as a surprise, and stimulated interest in spin as an important factor in high-energy hadronic interactions. Remarkable spin effects have been observed also in $pp$ elastic scattering beginning in 1978 [2]: the spin-parallel cross section was found to be four times larger than the spin-antiparallel one at large $p_T^2$. Spin effects were found to be large at the highest measured beam energies ($\sqrt{s} \leq 60$ GeV) and transverse momenta ($p_T \leq 4.5$ GeV/$c$), which contradicts the widespread idea that such effects should disappear at large transverse momenta and high energies [3]. The question, however, of what is a large enough $p_T$ and high enough energy still remains as an open question. Most of these results remain still unexplained.

In this talk I can cover only a small part of these findings. Given the limited size of this paper, I have also to exclude some of the results discussed in my talk. Here, I will concentrate mainly on inclusive processes in the beam fragmentation region (large $x_F$), in hyperon polarization, left–right pion asymmetries ($A_N$), and spin dependence and spin transfer in $\Lambda^0$ production. I will also briefly discuss the proton spin structure and the gluon polarization $\Delta G$. For more information see recent reviews [4,5].

The first polarized, low energy proton beams were obtained via scattering about 40 years ago. In the 1970's, after the development of polarized ion sources, the acceleration of polarized protons became possible, and first polarized proton and deuteron beams become available at the Zero Gradient Synchrotron (ZGS) at Argonne (ANL) with momenta up to 12 GeV/$c$ [6]. About 10 years later the Alternating Gradient Synchrotron (AGS) at Brookhaven (BNL) successfully accelerated polarized protons to a momentum of 22 GeV/$c$ [7], after solving the problem of avoiding intrinsic depolarizing resonances by simply jumping them.

Ten years ago, for the first time, high energy polarized proton and antiproton beams were obtained at 200 GeV/$c$ at Fermilab from the parity violating decay of $\Lambda^0$ and anti-$\Lambda^0$ hyperons [8] produced in a primary target by the 800 GeV/$c$ Tevatron proton beam. Decay protons are longitudinally polarized in the $\Lambda^0$ decay rest frame, and acquire a transverse polarization when Lorentz-boosted to the laboratory frame: larger the angle between the proton momentum vector and the $\Lambda^0$ direction in the decay frame, larger the transverse proton polarization in the laboratory frame. Those emitted near $\pm 90°$ in the $\Lambda^0$ rest frame have a transverse polarization of $\pm 64$ % in the laboratory frame. The polarized antiproton beam was obtained in a complementary way from the decay of anti-$\Lambda^0$ hyperons. Recently, a similar approach has been adopted at IHEP to produce a 40 GeV polarized proton beam.

In the inclusive measurement of $p \uparrow + N \rightarrow C \uparrow + X$ with the beam polarized transverse to the reaction plane, one can measure the analyzing power $A_N$, the depolarization (or polarization transfer) $D_{NN}$, and by averaging over opposite beam polarization states, the polarization $P_0$:

$$P_0 = \frac{\sigma(f = \uparrow) - \sigma(f = \downarrow)}{\sigma(f = \uparrow) + \sigma(f = \downarrow)}$$

$$A_N = \frac{1}{P_B} \cdot \frac{\sigma(i = \uparrow) - \sigma(i = \downarrow)}{\sigma(i = \uparrow) + \sigma(i = \downarrow)} \qquad D_{NN} = \frac{1}{P_B} \cdot \frac{\sigma(i = f) - \sigma(i \neq f)}{\sigma(i = f) + \sigma(i \neq f)}$$

where $P_B$ is the beam polarization normal to the production plane and $i$ ($f$) refers to initial (final) state polarization.

## 2 Hyperon Polarization

About 20 years ago at Fermilab it has been observed, that $\Lambda^0$ hyperons produced in $p + N \rightarrow \Lambda^0 + X$ at 300 GeV/$c$, emerged with a large, negative polarization [1] with respect to the normal to the production plane, and that the polarization increased in magnitude with increasing $x_F$ and $p_T$. This unexpected discovery set the stage for a systematic and detailed study of polarization effects in (inclusive) hyperon production.

Previous expectations, based on Regge theory and QCD predictions, were that spin effects would vanish at high energies, because of the smallness of spin-flip amplitudes, the large multiplicity of final states, and the contributions of several production channels to an inclusive process. These would make it

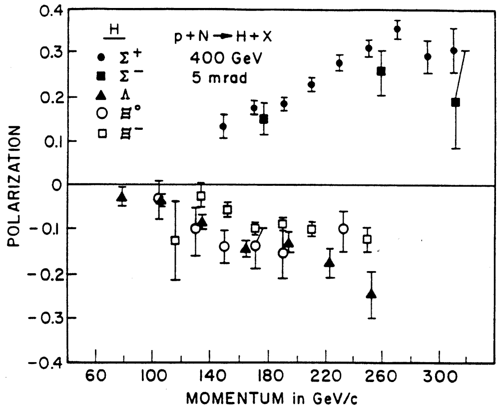


Figure 1: Polarization of different hyperons in $p + N \to Y + X$ as a function of their momentum $p_Y$. The hyperons are produced at a fixed angle of about 5 mrad with a 400 GeV/$c$ proton beam ($\langle x_F \rangle \sim p_Y/p_B$ and $\langle p_T \rangle \sim p_Y \times 0.005$.

unlikely to have the coherent interference between spin non-flip and spin flip amplitudes that would lead to sizable polarization effects.

Since then $\Lambda^0$ polarization experiments have covered a wide kinematic range of transverse momentum ($0 \le p_T \le 4.5$ GeV/$c$) [12], and a large incident beam momentum range from 1.5 GeV/$c$ to 800 GeV/$c$ in fixed target experiments and from $\sqrt{s} = 31$ to 62 GeV in colliding beam experiments, using a variety of beam particles and nuclear targets, both unpolarized. These experiments have shown that most hyperons are produced polarized. Figure 1 summarizes the polarizations of various hyperons produced around 5 mrad [13,14,15,16,17]. This plot can be considered already a *classic* in this field. For detailed and complete reviews, see ref. [9,10,11,4,5]. The main features of the hyperon polarization can be summarized as follows:

1. The polarization of the hyperons is normal to the production plane.
2. The magnitude of the polarization increases linearly with $p_T$, and reaches a plateau around $0.7 - 1.0$ GeV/$c$ above which it remains constant.
3. The magnitude of the polarization increases linearly with $x_F$.
4. The $\Lambda^0$ polarization is (almost) independent of the beam energy over the measured interval of $10 - 2000$ GeV/$c$.
5. There is a small (A–)dependence of the polarization on the target type.
6. Almost all hyperons are found to be polarized in the beam fragmentation region: $P_{\Sigma^0} \sim P_{\Sigma^+} \sim P_{\Sigma^-} \sim -P_{\Lambda^0} \sim -P_{\Xi^-} \sim -P_{\Xi^0}$, but $P_{\Omega^-} \sim 0$.

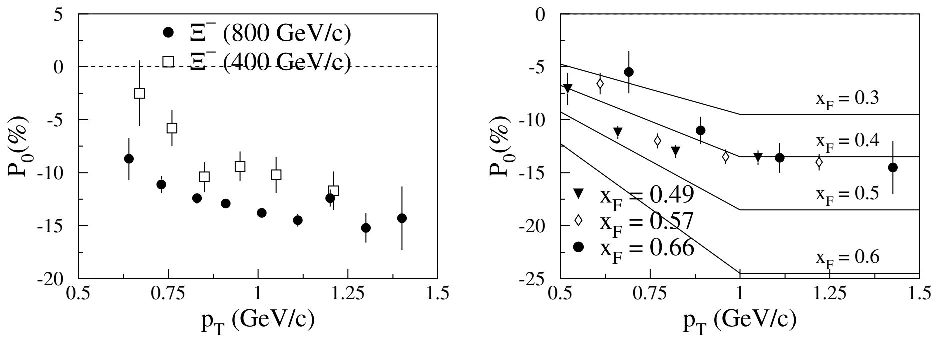


Figure 2: Energy dependence of the $\Xi^-$ polarization at 400 GeV/$c$ [15] and 800 GeV/$c$ [19]. $x_F$ / $p_T$ dependence of $\Xi^-$ $P_0$ (data points) [19] compared to $\Lambda^0$ $P_0$ (parametrization) [12].

7. Some anti-hyperons produced by protons are found to be polarized: $P_{\overline{\Lambda^0}} = 0$, but $P_{\overline{\Sigma^+}} \sim +10\%$ and $P_{\overline{\Xi^-}} \sim -10\%$.
8. There is a large correlation (spin transfer) between the incident beam polarization and outgoing hyperon.

As the energy range has increased, and the variety and amount of data has increased as well, these features have become more striking and suggestive of some simple underlying dynamical mechanism. While the data on other hyperons are not as extensive as for $\Lambda^0$, they are consistent with a similar kinematic behavior, but with differing signs and magnitudes of the polarization. Recent experiments have investigated these regularities: other hyperons do not exhibit such a striking and schematic behavior as does the$\Lambda^0$ polarization. These experiments show that the polarization of the $\Xi^-$ [19] increases and that of the $\Sigma^+$ [20] decreases with energy, and that it does not follow the simple $x_F$ / $p_T$ pattern typical of the $\Lambda^0$ polarization. Figure 2 summarizes the behavior of the $\Xi^-$ polarization [19].

The features of the $\Lambda^0$ polarization have led to the idea that polarization is primarily a leading particle effect, that is, the polarization is a consequence of the beam proton fragmentation mechanism. Thus there should be no polarization for particles that do not share any quarks with the incoming projectile, such as $\Omega^-$ and anti-hyperons. Indeed, it has been observed that $\Omega^-$ and anti-$\Lambda^0$ produced by protons are not polarized [18,12]. Against all expectations, however, large polarizations have been found for anti-$\Xi^-$ [21] and anti-$\Sigma^+$ [22] produced with protons as shown in Fig. 3.

Different quark parton models have been proposed to interpret these polarization effects by introducing spin dependent asymmetries into the quark

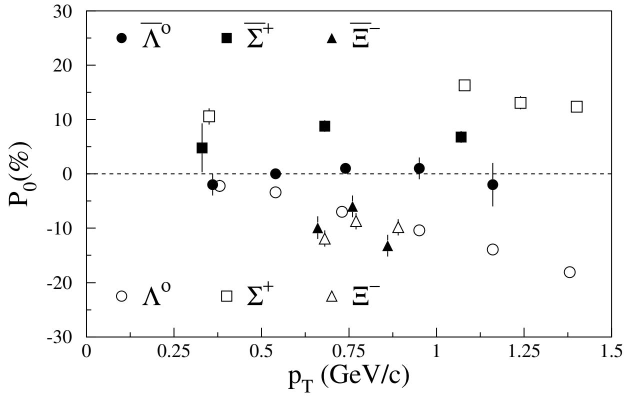


Figure 3: Polarization of anti-hyperons produced by protons: $\overline{\Lambda^0}$ [18], $\overline{\Sigma+}$ [22], and $\overline{\Xi^-}$ [21]. For comparison are shown the polarizations of hyperons from the same experiments.

and di-quark production and scattering amplitudes. Since the first results on hyperon polarization, its origin has been discussed in terms of highly polarized *strange* quarks, which, by mechanisms based on semiclassical arguments like the Lund string model [23] or based on the Thomas precession [24], or inspired by QCD [25], acquire a large negative polarization in the fragmentation process, before recombining with the beam proton remnant to give a polarized hyperon. The sign of the polarization depends on the SU(6) spin-flavor structure of the hyperon.

More about the mechanisms responsible for the polarization phenomena can be learned by extending these studies to heavier baryons – $\Lambda_c^+$ for instance, where the mass of the *charmed* quark can differentiate between polarization effects in fragmentation (low $P_0$) and in recombination (high $P_0$). The $c-$baryon sector has not been explored yet. There exist some evidences that the $\Lambda_c^+$ is produced with large, positive polarization [26].

## 3 Inclusive Meson Production with Polarized (Anti)Proton Beams

An other interesting and puzzling chapter of *spin effects* in hadronic interactions are the transverse single spin asymmetries $A_N$ (analyzing power) in inclusive hadron production. In these experiments one measures the right–left production asymmetry with respect to the direction of the beam polarization. For instance, a value of 0.33 for $A_N$ indicates that twice as many particles are produced to the left than to the right with a spin-up beam.

Several experiments have studied the transverse spin asymmetry $A_N$ in

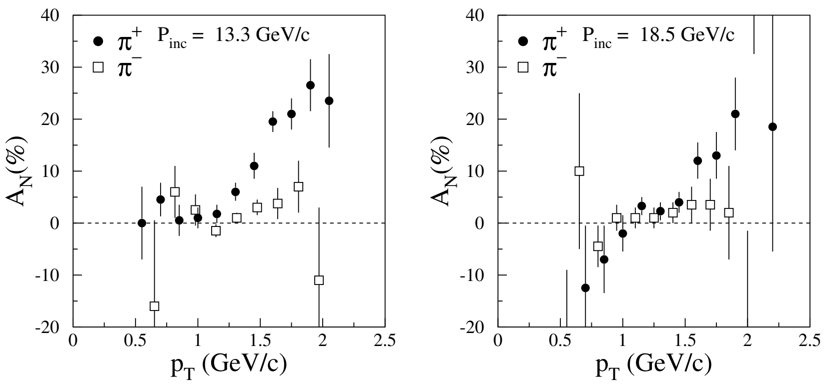


Figure 4: $A_N$ in inclusive pion production at two different beam energies from BNL [28].

inclusive hadron production using either polarized (anti-)proton beams or polarized targets. With an unpolarized beam and a polarized target, experiments have found small asymmetries in the beam fragmentation region, which suggests a strong leading effect for $A_N$ similar to that proposed for the hyperon polarization. Naively, in simple quark fragmentation models, $A_N$ can be seen as the memory of the recombining valence quark on the beam polarization.

The first measurements of $A_N$ for $\pi^+$ and $pi^-$ production were performed at ANL [27], where sizable asymmetries were observed in the forward beam fragmentation direction (large $x_F$). Figure 4 shows $A_N$ for inclusive $\pi^\pm$ production at relatively low values of $x_F$ ($\langle x_F \rangle \sim 0.2$) as a function of $p_T$ from another experiment at BNL [28] at two different incident beam momenta. This experiment have not observed any $x_F$ dependence of $A_N$ in the range $0.0 < x_F < 0.4$. Similar measurements have been performed ore recently at IHEP at 40 GeV/$c$ in the same kinematical region also for kaon and proton inclusive production [29]. The outcome of the IHEP experiment is consistent to the BNL results.

Analyzing power measurements with the 200 GeV/$c$ transversely polarized proton and antiproton beams at FNAL for $\pi^\pm$ mesons are presented in Fig. 5 and Fig. 6. The $A_N$ results for $\pi^\pm$ produced by protons (Fig. 5) [30] show a striking mirror symmetric dependence in $x_F$, where $A_N$, with increasing $x_F$, increases to large positive values for $\pi^+$'s and decreases to large negative values for $\pi^-$'s. A threshold for the onset of the asymmetry is observed around $p_T \sim$ 0.5 GeV/$c$, below which $A_N$ is essentially zero, and above which $A_N$ increases (decreases) with $p_T$ up to $p_T \sim 1.0$ GeV/$c$ for $\pi^+$'s ($\pi^-$'s) in the covered $p_T$ range. The data suggest a possible saturation of $A_N$ for $p_T \sim 1.0$ GeV/$c$ similar to that observed for the hyperon polarization, however the measured

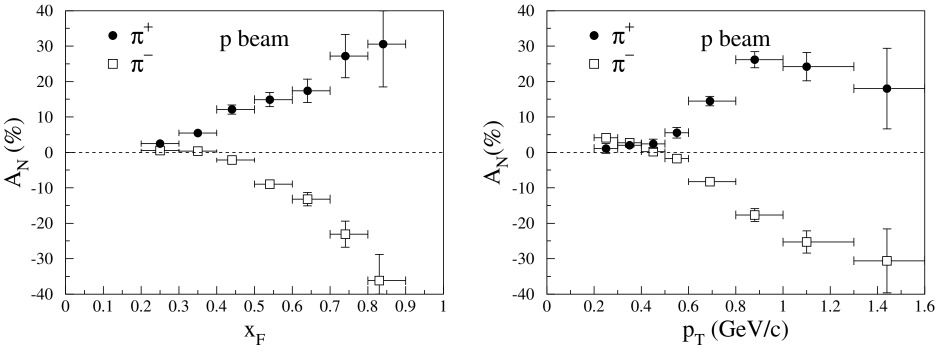


Figure 5: $A_N$ in $p\uparrow + p \to \pi^+/\pi^- + X$ at 200 GeV/$c$ from FNAL [30].

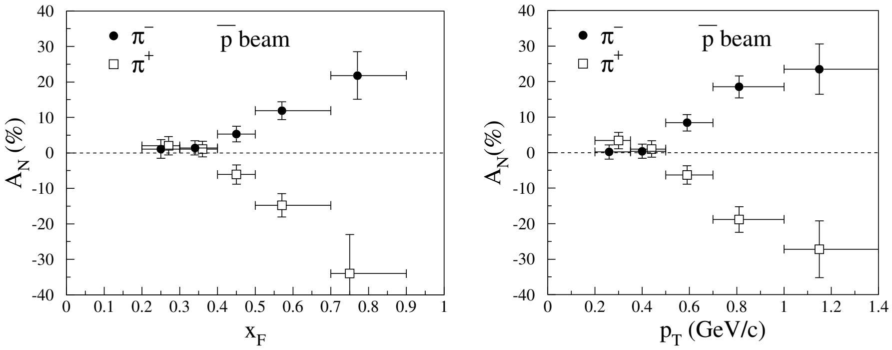


Figure 6: $A_N$ in $\bar{p}\uparrow + p \to \pi^+/\pi^- + X$ at 200 GeV/$c$ from FNAL [32].

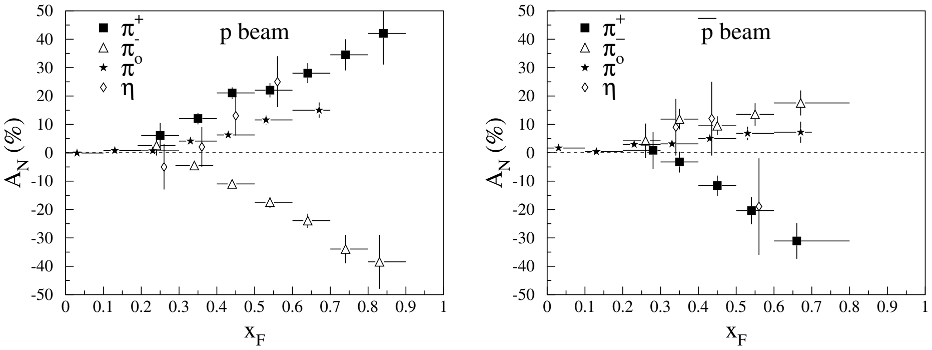


Figure 7: $A_N$ in $p\uparrow/\bar{p}\uparrow + p \to \pi^+/\pi^-/\pi^0/\eta + X$ at 200 GeV/$c$ over the same $p_T$ interval of $0.7 \le p_T \le 2.0$ GeV/$c$ from FNAL [30,31,32,33].

$p_T$ interval does not extend enough in the $p_T$ to reach a definite conclusion on this point.

A charge symmetric behavior is also found for $\pi^{\mp}$'s produced with the polarized antiproton beam (Fig. 6) [32]. Here $A_N$ increases with increasing $x_F$ to large positive values for $\pi^-$'s and decreases with increasing $x_F$ to large negative values for $\pi^+$'s. The data show a similar $p_T$ dependence as for the proton beam, in particular also here a threshold for the onset of the asymmetry is observed around $p_T \sim 0.5$ GeV/$c$.

The $A_N$ results for different mesons are summarized in Fig. 7 [30,31,32,33]. These results show a similar kinematical $x_F$ and $p_T$ dependence for the different mesons, in which $A_N$ increases in magnitude with $x_F$ to large values above a threshold of about 0.5 GeV/$c$ in $p_T$. $A_N$ for $\pi^0$ is only half as large as for the charged pions, and the sign of $A_N$ for $\pi^0$ produced either by polarized protons or antiprotons is the same. For any fixed $x_F$ and $p_T$ they can be summarized as follows:

$$A_N(p\uparrow p \to \pi^+ + X) \sim -A_N(p\uparrow p \to \pi^- + X) \sim \tfrac{1}{2}A_N(p\uparrow p \to \pi^0 + X) > 0$$
$$A_N(\bar{p}\uparrow p \to \pi^- + X) \sim -A_N(\bar{p}\uparrow p \to \pi^+ + X) \sim \tfrac{1}{2}A_N(\bar{p}\uparrow p \to \pi^0 + X) > 0$$
$$A_N(p\uparrow p \to \pi^+ + X) \sim A_N(\bar{p}\uparrow p \to \pi^- + X) > 0$$
$$A_N(p\uparrow p \to \pi^- + X) \sim A_N(\bar{p}\uparrow p \to \pi^+ + X) < 0$$
$$A_N(p\uparrow p \to \pi^0 + X) \sim A_N(\bar{p}\uparrow p \to \pi^0 + X) > 0$$

Recently, $\pi^-$ production has been studied around 25 GeV/$c$ at BNL [34]. The primary goal of this experiment has been to develop a proton polarimeter based on the $pi^-$ production asymmetry. Altough data have been taken only over a small $x_F$ interval centered around $x_F \sim 0.5$, they show a $p_T$ dependence similar to the one measured at FNAL with the 200 GeV/$c$ polarized proton beam, thus suggesting a possible energy independence of the effect, as in the case of $\Lambda^0$ polarization.

*Do we understand these phenomena or how does an experimentalist look at them:* The pion $A_N$ results at large $x_F$ can be explained qualitatively as an effect similar to that proposed to explain the hyperon polarization [24], in which $q\bar{q}$ pairs produced in the fragmentation process become transversally polarized and at large $x_F$ the transverse spin of the (anti)protons is correlated to its (anti)quark constituents. To produce a spin-zero meson, the polarized produced $(q)\bar{q}$ will couple with the spectator (anti)*up* or (anti)*down* quark from the polarized (anti)proton beam only in an antiparallel configuration. The reflected sign of $\pi^-$'s with respect to $\pi^+$'s (and between $\bar{p}$ and $p$ beams) may originate from the fact that the *up* (anti)quark spin is almost fully aligned with that of the (anti)proton for $x_F$ approaching one, whereas that of the *down* (anti)quark is oppositely aligned. This conclusion is consistent with recent SMC results [35] on semi-inclusive deep inelastic scattering, which probed the polarization of valence quarks in the nucleon. These asymmetries represent the first evidence on transversity.

## 4 $\Lambda^0$ Spin Observables and Spin Transfer

A natural extension of the hyperon polarization measurements, performed with unpolarized beams and targets, is the study of the hyperon production with polarized proton beams in similar kinematical conditions. These studies may lead to more insight into the mechanism of the polarization effects. In the reaction $p\uparrow p \rightarrow \Lambda^0 + X$ several spin observables can be measured, in particular the production asymmetry $A_N$ and the polarization transfer or depolarization $D_{NN}$.

First measurements of the $\Lambda^0$ spin observables were carried out at ANL with the 6 GeV/$c$ polarized proton beam more than 20 years ago [36]. The outcome of the experiment is that there is *structure* in all 3 spin parameters for $x_F > 0.8$. At lower $x_F$ these results do not indicate large spin effects within measurement errors. However, this energy is still too small to compare these measurements with the results on the $\Lambda^0$ polarization discussed above.

The $\Lambda^0$ spin parameters have been measured at AGS at 13.8 GeV/$c$ and 18.5 GeV/$c$ in the central and small $x_F$ regions [37,38], where spin effects are expected to be small. Figure 8 shows the $A_N$ and $D_{NN}$ results at 18.5 GeV/$c$ as a function of $x_F$ for different $p_T$ intervals. These measurements are compatible with zero, and no $p_T$ dependence is observed. On the contrary, $D_{NN}$ in $\Sigma^0$ production was found to be as large as 25 % [38].

More recently, $\Lambda^0$ production has been studied with the 200 GeV/$c$ polarized proton beam at FNAL. The $\Lambda^0$ $A_N$ data obtained with this facility are shown in Fig. 9 [39] as a function of $x_F$ and $p_T$. They indicate substantial negative values of the analyzing power, in which $A_N$ increases in magnitude with $x_F$ and $p_T$, and reaches values larger than $-15$ % at large $x_F$ and $p_T$, while at low $x_F$ and/or low $p_T$ these results are compatible with zero. The trend of these results shows a similar behavior as the existing $\Lambda^0$ polarization data, thus suggesting a common interpretation.

The depolarization $D_{NN}$ is shown in Fig. 10 [40]. At large $x_F$, $D_{NN}$ reaches positive values as large as 30 % at $p_T \sim 1$ GeV/$c$, while almost no dependence in $x_F$ is observed for $x_F < 0.5$, where $D_{NN}$ is slightly positive. $D_{NN}$ grows to significantly large positive values with increasing $p_T$ and a possible saturation in $p_T$ is seen around 1.0 GeV/$c$, while at low $p_T$ values $D_{NN}$ is compatible with zero. Also these data show a kinematical behavior similar to the $\Lambda^0$ $P_0$ and $A_N$ results. These FNAL results are consistent with the BNL data in the overlapping kinematic region at low $x_F$, where both are compatible with zero.

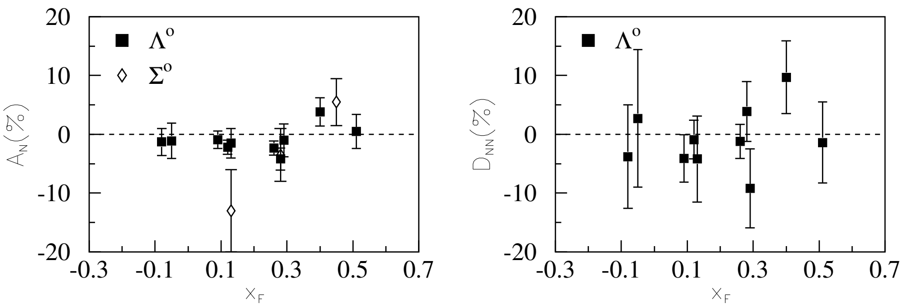


Figure 8: $A_N$ and $D_{NN}$ in inclusive $\Lambda^0$ [37] and $\Sigma^0$ [38] production at 18.5 GeV/$c$ from BNL.

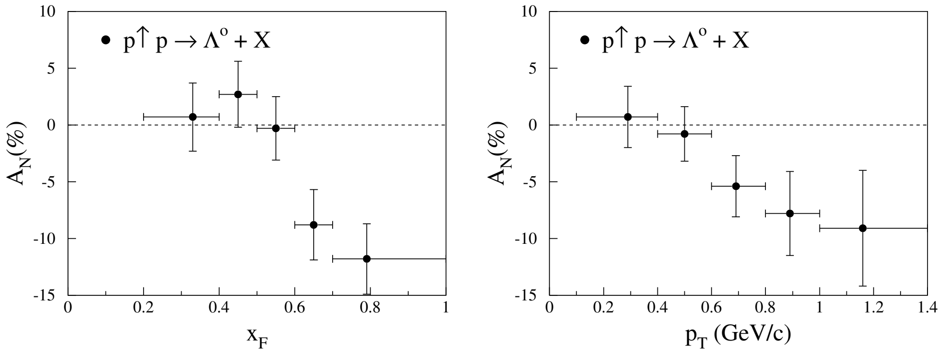


Figure 9: Analyzing power in inclusive $\Lambda^o$ production at 200 GeV/$c$ from FNAL [39].

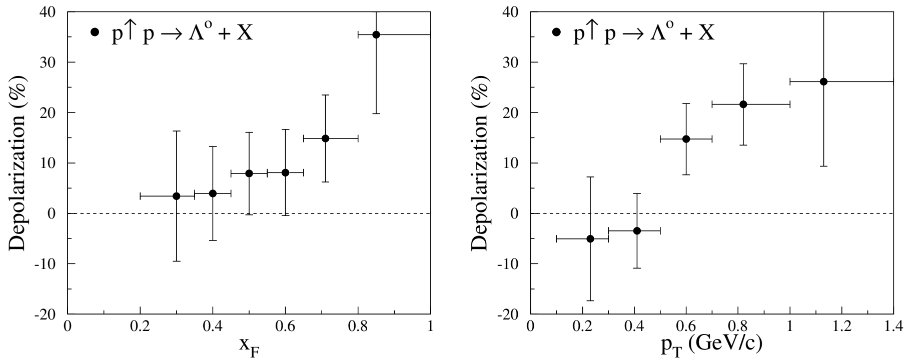


Figure 10: $D_{NN}$ in inclusive $\Lambda^0$ production at 200 GeV/$c$ from FNAL [40].

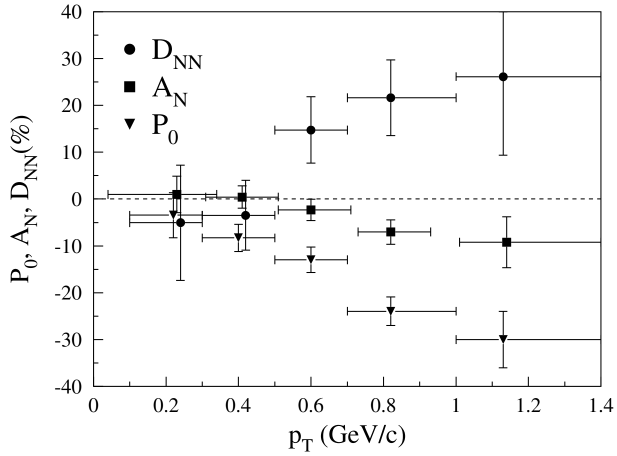


Figure 11: Spin observables in $p \uparrow p \to \Lambda^0 + X$ at 200 GeV/$c$ from FNAL.

The large positive $D_{NN}$ values indicate a sizable spin transfer (as large as 30 %) from the incident polarized proton to the outgoing $\Lambda^0$. Large spin transfers in hyperon production have been also observed in inclusive $\Xi^-$ and $\Omega^-$ production by a neutral beam containing also transversely polarized $\Lambda^0$'s and $\Xi^0$'s [42,43]. Unfortunately, the amount of this spin transfer has been never quantified. The spin transfer in the latter reactions is more easily interpreted in quark models, since a polarized valence *strange* quark from the incoming polarized hyperon is transferred to the outgoing hyperon which is also polarized, while in the former process ($p \uparrow p \to \Lambda^0 + X$) there are no polarized valence *strange* quarks in the incident polarized proton.

Figure 11 is my favorite plot concerning *spin effects* in inclusive $\Lambda^0$ production. It summarizes the 3 spin observables discussed so far. All data shown were taken in the same kinematical region and simultaneously (experiment E704 at FNAL) [41], therefore allowing for a straightforward comparison of $P_0$, $A_N$, and $D_{NN}$. All 3 spin parameters show a similar $p_T$ dependence, but with different signs and magnitudes, in which the asymmetries increase with $p_T$:

$$P_0 \sim -\, D_{NN} \sim \frac{1}{3} A_N < 0 \, .$$

In most of the quark models proposed so far to explain the $\Lambda^0$ polarization, the $\Lambda^0$ spin is carried by its constituent *strange* quark while the *ud* di-quark is in a spin and isospin singlet state (SU(6) wave functions). Therefore, no correlation with the incident proton polarization is expected in $\Lambda^0$ production, since the $ud$ di-quark propagates unperturbed as a spectator in the interaction, and spin asymmetries related to the beam polarization should vanish. The large negative $\Lambda^0$ production asymmetry $A_N$ [39] and the large positive spin transfer $D_{NN}$ [40] at large $x_F$ are difficult to integrate in this picture and cannot be attributed to an effect similar to that proposed to explain the $\Lambda^0$ polarization, where a highly polarized *strange* quark produced in the fragmentation process recombines with an unpolarized $ud$ spectator di-quark from the incident proton independently of its polarization. It appears that also the spectator di-quarks play a more active role in the production process, which was underestimated, if not completely neglected [44].

## 5 What about the Nucleon Spin Structure and $\Delta G$ ?

The nucleon spin structure has been studied mainly in deep inelastic scattering (DIS) of polarized leptons off polarized nucleons. For a review, see the talk of [45]. Experiments have shown that quark spins contribute little to the nucleon spin, thus implying an appreciable contribution either from gluon spins or possibly from orbital angular momentum. The gluon polarization $\Delta G$ can be accessed directly in reactions, where the gluons enter in the initial state of the hard scattering sub-process at lowest order in $\alpha_s$, like open charm or di-jet production in polarized DIS. $\Delta G$ can be also accessed in polarized proton proton collisions at high c.m. energies, by studying, for example, di-jet, direct photon, or heavy flavor production. Polarized proton collisions allow also to access $\Delta u$, $\Delta d$, and $\Delta s$ via $W^\pm$ and $Z^0$ production. For a review of the spin physics potential of a polarized proton collider (RHIC), see the talk of [46].

The first attempt to access the gluon polarization $\Delta G$ was done at Fermilab at the polarized proton beam facility with a polarized pentanol target [47]. Di-jet type events were tagged by multi-$\gamma$ pairs. The multi-$\gamma$ is a set of $\gamma$-rays detected in an electromagnetic calorimeter covering the 90° c.m. angle, and the multi-$\gamma$ pair are two multi-$\gamma$ detected in both parts of the calorimeter located to the left and to the right of the beam axis. Most of the multi-$\gamma$ pairs come from di-jet type events, and represent their electromagnetic component. Two kinematical variables were used to study these events: the pseudo mass $M' = |p_T^{\gamma 1}| + |p_T^{\gamma 2}|$ ($M' \propto\sim 2\,\hat{s}$) and the transverse momentum $p_T^\gamma = |p_T^{\gamma 1}| - |p_T^{\gamma 2}|$, where $p_T^{\gamma i}$ are the transverse momenta of each multi-$\gamma$. Events were selected by requiring $M' > 2$ GeV/$c$ and $|p_T^\gamma| < 1$ GeV/$c$. That is equivalent to require that the multi-$\gamma$ were produced at 90° in the c.m. opposite in azimuth with a large c.m. energy $\hat{s}$, which is characteristic of a di-jet type events. MonteCarlo studies of this process showed that gluon-gluon fusion, quark-gluon scattering and quark-antiquark annihilation contribute about 45 %, 45 %, and 10 %, respectively, to multi-$\gamma$ events. Thus this process, despite the still low c.m. energy, is rather sensitive to the gluon terms in the underlying partonic interactions, and the double spin asymmetry $A_{LL}$, with an analyzing power $\hat{a}_{LL}$ of $\sim 0.3$, is sensitive to the gluon polarization $\Delta G/G$.

Figure 12 shows the double-spin asymmetry $A_{LL}$ for inclusive multi-$\gamma$ pair production as a function of the pseudo mass $M'$. The $A_{LL}$ values do not deviate significantly from zero within statistical uncertainties (the shaded area is the average of the individual measurements). These data represent the first experimental result, which is sensitive to the gluon polarization in the nucleon. The small value of $A_{LL}$ suggests a small gluon polarization $\Delta G$. Indeed, theoretical models which predict small or zero gluon polarization agree better with these data than those which predict a very large $\Delta G$. In other words, these data favor a small $\Delta G$ in the $x$ range $0.05 < x < 0.35$.

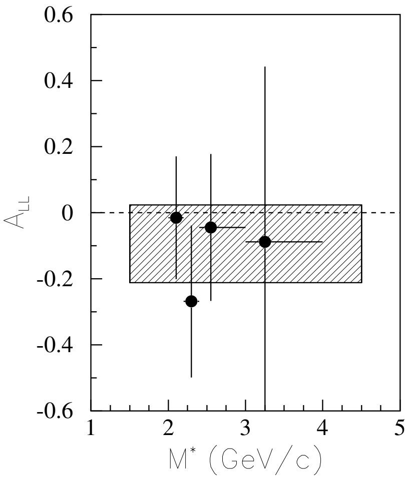


Figure 12: $A_{LL}$ for inclusive multi-$\gamma$ pair production [47]. The hatched area shows the mean value of the data points.

◊ ◊ ◊ ◊ ◊ ◊ ◊ ◊ ◊

Transverse spin studies in inclusive reactions continue to yield rich and puzzling results. The similarity of the $x_F$ and $p_T$ kinematical dependencies of the spin asymmetries in various processes suggests a common origin and explanation for the observed phenomena. On the contrary, no quantitative theoretical explanation, which is consistent with all these phenomena, exists yet, and the prevailing theory of hadronic structure and interactions, QCD, predicts zero polarization at high energies and transverse momenta [3]. No trend toward zero polarization, however, is observed in the present data, even at the highest measured $p_T$, where one might hope that perturbative QCD should be applicable.

Recently, models based on non-perturbative approaches and peripheral mechanisms with an underlying quasi-binary sub-process, such as the *soft* $\pi$ exchange mechanism [48], or resonance-decay interference between real and virtual channels [49], have been proposed to explain the $\Lambda^0$ polarization. The pion asymmetries have been successfully fit with pQCD inspired models by taking into account higher twist effects and the quark intrinsic motion $k_T$ [50]. Models, based on the idea of rotating constituents in polarized protons and associated production have been also proposed [51], and they appear to be in qualitative agreement with the features of the pion and $\Lambda$ data. For more information on the current status of the theoretical understanding and recent developments see the talks of [52,53,54] at this conference.

New and exiting spin effects in hadronic interactions in a new energy domain, which will give also direct access to the nucleon spin structure, are expected soon from the upcoming polarized proton collider at BNL [46].

## References


1. G. Bunce *et al.*, Phys. Rev. Lett. **36** (1976) 1113.
2. D.G. Crabb *et al.*, Phys. Rev. Lett. **41** (1978) 1257.
3. G.L. Kane, J. Pumplin, and W. Repko, Phys. Rev. Lett. **41** (1978) 1689.
4. A. Bravar, in *Trends in Collider Spin Physics, Trieste 1995*, edited by Y. Onel, N. Paver, and A. Penzo (World Scientific Publishing, 1997).
5. S.B. Nurushev, Int. J. Mod. Phys. A **12** (1997) 3433.
6. A. Yokosawa, Phys. Rep. **64** (1980), 47.
7. F.Z. Khiari *et al.*, Phys. Rev. D **39** (1989) 45.
8. D.P. Grosnick *et al.*, Nucl. Inst. Meth. Phys. Res. A **290** (1990) 269.
9. L.G. Pondrom, Phys. Rep. **122** (1985), 57.
10. K. Heller, in *Spin96, Amsterdam 1996*, edited by C.W. de Jager *et al.* (World Scientific Publishing, 1997).
11. A.D. Panagiotou, Int. J. Mod. Phys. A **5** (1990) 1197.
12. B. Lundberg *et al.*, Phys. Rev. D **40** (1989) 3557.
13. K. Heller *et al.*, Phys. Rev. Lett. **51** (1983) 2025.
14. Y. Wah *et al.*, Phys. Rev. Lett. **55** (1985) 2551.
15. R. Rameika *et al.*, Phys. Rev. D **33** (1986) 3172.
16. C. Wilkinson *et al.*, Phys. Rev. Lett. **58** (1987) 855.
17. E.C. Dukes *et al.*, Phys. Lett. B **193** (1987) 135.
18. K. Heller *et al.*, Phys. Rev. Lett. **41** (1978) 607.
19. J. Duryea *et al.*, Phys. Rev. Lett. **67** (1991) 1193.
20. A. Morelos *et al.*, Phys. Rev. D **52** (1995) 3777.
21. P.M. Ho *et al.*, Phys. Rev. Lett. **65** (1990) 1713.
22. A. Morelos *et al.*, Phys. Rev. Lett. **71** (1993) 2172.
23. B. Andersson *et al.*, Phys. Lett. B **85** (1979)417.
24. T.A. Degrand and H.I. Miettinen, Phys. Rev. D **23** (1981) 1227; **24** (1981) 2419; **31** (1985) 661(E).
25. W.G.D. Dharmaratna and G.R. Goldstein, Phys. Rev. D **41** (1990), 1731; J. Szwed, Phys. Lett. B **105** (1981), 403;

T. Fujita and T. Matsuyama, Nihon University Report NUP-A-879, 1987.
26. A.N. Aleev *et al.*, Yad. Fiz. **43** (1986) 619;
P. Chauvat *et al.*, Phys. Lett. B **199** (1987) 304.
27. W.H. Dragoset *et al.*, Phys. Rev. D **18** (1978) 3939.
28. S. Saroff *et al.*, Phys. Rev. Lett. **64** (1990) 995.
29. V.V. Abramov *et al.*, Nucl. Phys. B **492** (1997) 3.
30. D.L. Adams *et al.*, Phys. Lett. B **264** (1991) 462.
31. D.L. Adams *et al.*, Phys. Lett. B **261** (1991) 201.
32. A. Bravar *et al.*, Phys. Rev. Lett. **77** (1996) 2626.
33. D.L. Adams *et al.*, Nucl. Phys. B **510** (1998) 3.
34. Y.I. Makdisi, these proceedings.
35. B. Adeva *et al.*, Phys. Lett. B **420** (1998) 180.
36. A. Lesnik *et al.*, Phys. Rev. Lett. **35** (1975) 770.
37. B.E. Bonner *et al.*, Phys. Rev. D **38** (1988) 729.
38. B.E. Bonner *et al.*, Phys. Rev. Lett. **62** (1989) 1591.
39. A. Bravar *et al.*, Phys. Rev. Lett. **75** (1995) 3073.
40. A. Bravar *et al.*, Phys. Rev. Lett. **78** (1997) 4003.
41. A. Bravar *et al.*, to be submitted to Phys. Rev. D.
42. H.T. Diehl *et al.*, Phys. Rev. Lett. **67** (1991) 804.
43. D.M. Woods *et al.*, Phys. Rev. D **54** (1996) 6610.
44. M. Anselmino, P. Kroll, and B. Pire, Z. Phys. C **36** (1987), 89;
P. Kroll and W. Schweiger, Nucl. Phys. A **474** (1987), 608.
45. E. Gabathuler, *Experimental Review of Nucleon Spin*, these proceedings.
46. S. Vigdor, *Program of Spin Studies at RHIC*, these proceedings.
47. D.L. Adams *et al.*, Phys. Lett. B **336** (1994) 269.
48. J. Soffer and N.A. Törnqvist, Phys. Rev. Lett. **68** (1992) 907.
49. R. Barni, G. Preparata, and P.G. Ratcliffe, Phys. Lett. B **296** (1992) 251.
50. M. Anselmino, M. Boglione, and F. Murgia, Phys. Lett. B **362** (1995) 164.
51. L. Zuo-tang and C. Boros, Phys. Rev. Lett. **79** (1997), 3608;
C. Boros, L. Zuo-tang, and M. Ta-chung, Phys. Rev. D **51** (1995), 4867.
52. P.G. Ratcliffe, *Theory of Spin Effects in Hadronic Reactions*, these proceedings.
53. F. Murgia, *Single Spin Asymmetries in pp and $\bar{p}p$ Inclusive Processes*, these proceedings.
54. L Zuo-tang, *Hyperon Polarization and Single-Spin Asymmetries in Different Hadronic Processes*, these proceedings.